CHEMISTRY
A EUROPEAN JOURNAL

DOI: 10.1002/chem.200700826

Synthesis and Metal Complexes of Chiral C_2-Symmetric Diamino–Bisoxazoline Ligands

Geoffroy Guillemot,[a] Markus Neuburger,[b] and Andreas Pfaltz*[a]

Abstract: A synthetic route to tetradentate chiral N_4 ligands has been developed with the aim to study the potential of corresponding iron and manganese complexes as catalysts for enantioselective epoxidation. These ligands, which contain two oxazoline rings and two trialkylamino groups as coordinating units, are readily prepared in enantiomerically pure form by the reaction of chiral 2-chloromethyloxazolines with achiral *N*,*N*′-dimethylethane-1,2-diamine or chiral (*R*,*R*)-*N*,*N*′-dimethylcyclohexane-1,2-diamine. The ligands derived from *N*,*N*′-dimethylethane-1,2-diamine reacted with anhydrous metal halides $MnCl_2$ and $FeCl_2$ in a stereoselective manner to give octahedral mononuclear complexes that have the general formula Δ-[(L)MCl_2]. In contrast, the ligands derived from *N*,*N*′-dimethylcyclohexane-1,2-diamine formed complexes with different coordination modes depending on the diastereomer employed: in one case the metal ion was found to be pentacoordinate, in the other case a hexacoordinated complex was observed. The structure of a series of Fe and Mn complexes was determined by X-ray analysis. The coordination chemistry of these ligands was further studied by X-ray and NMR analyses of the diamagnetic isostructural complexes [(L)$ZnCl_2$]. Analogous ionic complexes, which were prepared by removing chloride with silver trifluoromethanesulfonate or hexafluoroantimonate, were tested as catalysts for the epoxidation of olefins.

Keywords: chiral ligands · iron · manganese · N ligands · oxazolines

Introduction

Iron and manganese complexes with nitrogen ligands have been extensively studied as models of active sites of monooxygenases and as oxidation catalysts for organic synthesis.[1–5] To mimic metal porphyrins such as cytochrome P-450,[2] which play a central role in many biological processes, a variety of synthetic ligands were developed. Two of the most widely used classes of ligand are the porphyrins[4] and tetradentate Schiff base derivatives,[5] exemplified in Figure 1 by [Mn(tpp)] and [Mn(salen)] complexes [tpp: tetraphenylporphyrin dianion; salen: *N*,*N*′-ethylene-bis(salicylideneiminato) dianion]. With the growing importance of asymmetric catalysis, many efforts have been made to devise chiral variants of these ligands, the most successful examples are the chiral Mn(salen) catalysts for the epoxidation of unfunctionalized olefins.[6]

More recently, inspired by the remarkable oxidative properties of non-heme iron enzymes such as methane monooxygenase[7] or Rieske dioxygenases,[8] more flexible N_4 ligands containing sp^3-hybridized N atoms have been synthesized. In particular, Fe and Mn complexes derived from *N*,*N*′-dimethyl-*N*,*N*′-bis(2-pyridylmethyl)ethane-1,2-diamine (bpmen) and (*R*,*R*)-*N*,*N*′-dimethyl-*N*,*N*′-bis(2-pyridylmethyl)cyclohexane-1,2-diamine [(*R*,*R*)-bpmcn] have emerged as efficient catalysts for the epoxidation of certain olefins.[9,10] However, attempts to use bpmcn or other chiral ligands of this type for enantioselective epoxidation have met limited success.[9a,11]

In connection with our work on chiral oxazoline-based ligands[12,13] we have prepared a series of N_4 ligands that are structurally related to bpmen and bpmcn, but contain two oxazoline instead of pyridine rings. Here we report the synthesis of (*S*,*S*)-bomen and (*S*,*R*,*R*,*S*)-bomcn (Figure 1) ligands, the preparation and structure of various metal complexes and preliminary epoxidation studies using manganese and iron catalysts derived from these ligands.

Ligands of this type have several attractive features: i) they possess a relatively simple C_2-symmetric structure

[a] Dr. G. Guillemot, Prof. Dr. A. Pfaltz
Department of Chemistry, University of Basel
St. Johanns-Ring 19, 4056 Basel (Switzerland)
Fax: (+41) 61-267-1103
E-mail: andreas.pfaltz@unibas.ch

[b] M. Neuburger
Laboratory for Chemical Crystallography, University of Basel
Spitalstrasse 51, 4056 Basel (Switzerland)

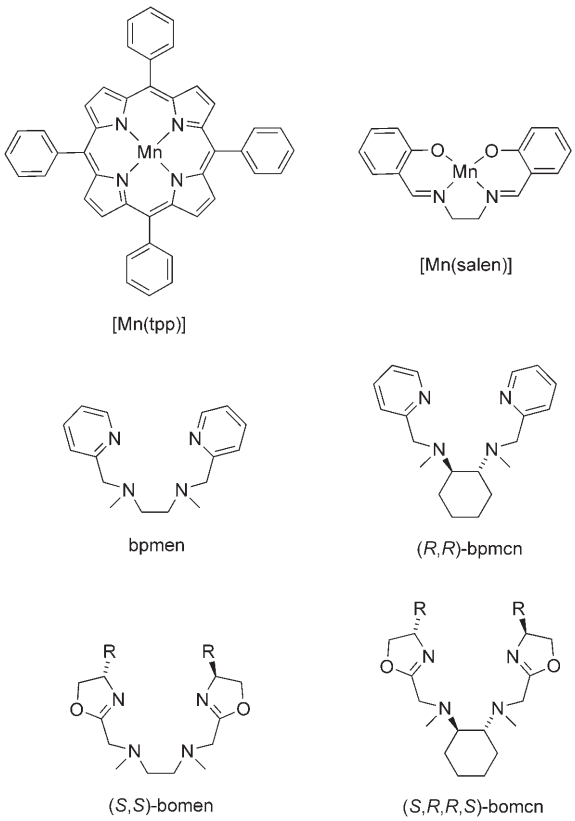

Figure 1. Structures of porphyrin, salen, and pyridine- and oxazoline-derived N_4 ligands.

and are readily assembled from commercially available enantiomerically pure amino alcohols; ii) the steric properties and conformational flexibility can be tuned by variation of the diamine bridge; iii) introduction of a chiral backbone like *trans*-cyclohexane-1,2-diamine allows further variation of the stereochemical properties; iv) the steric constraints generated by the substituents at the oxazoline rings provide a means for controlling the stereochemistry of metal complex formation. In this way the number of possible isomers that can arise through coordination to a octahedral metal center can be reduced.

Results and Discussion

Ligands synthesis and complex formation: 2-Chloromethyloxazolines **6a** and **6b** were chosen as the central intermediates in this synthesis, because they readily react with secondary diamines to afford the desired tetradentate ligands. Among the various possible routes to these intermediates[14–17] we investigated the two synthetic sequences shown in Scheme 1. Amide formation from chloroacetyl chloride and amino alcohol **2a** or **2b**, and subsequent cylization using Burgess' reagent afforded the chloromethyloxazolines **6a** and **6b** in 42–59% overall yield.[18] The alternative route, starting from chloroacetonitrile, also comprised two steps and led to the desired oxazolines **6a** and **6b** in similar overall yields (52–59%). However, the latter route is more

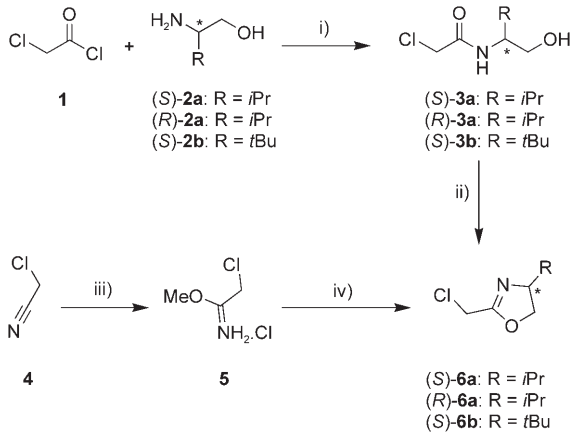

Scheme 1. Synthesis of 2-chloromethyl-2-oxazoline **6a** and **6b**. i) NEt_3, CH_2Cl_2, −20 °C, (83–89%); ii) Burgess reagent, THF, reflux, (51–66%); iii) MeOH, Et_2O·HCl, (>95%); iv) amino alcohol **2**, CH_2Cl_2, RT, (55–62%).

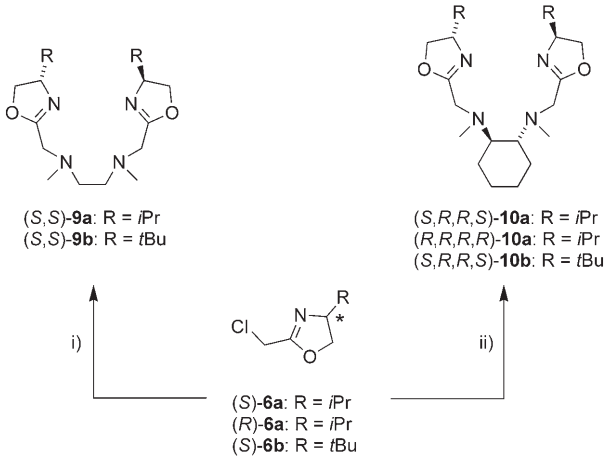

Scheme 2. Synthesis of bisoxazoline ligands **9** and **10**. i) *N*,*N*′-dimethylethane-1,2-diamine, K_2CO_3, CH_3CN, reflux; ii) (*R*,*R*)-*N*,*N*′-dimethylcyclohexane-1,2-diamine, K_2CO_3, CH_3CN, reflux, (39–51%).

attractive, as it involves less expensive, simpler reagents, and because different oxazolines can be prepared from chloroacetimidate hydrochloride **5** as a common precursor.

The 2-chloromethyloxazoline derivatives **6a** and **6b** were converted to the corresponding ligands **9a**, **9b**, **10a** and **10b** by treatment with *N*,*N*′-dimethylethane-1,2-diamine (**7**) or (*R*,*R*)-*N*,*N*′-dimethylcyclohexane-1,2-diamine (**8**), respectively, and anhydrous K_2CO_3 in acetonitrile under reflux (Scheme 2).[19] NMR analysis of the crude products showed essentially quantitative formation of the desired ligands. Ligands (*S*,*R*,*R*,*S*)- and (*R*,*R*,*R*,*R*)-**10a** and (*S*,*R*,*R*,*S*)-**10b** were purified by flash chromatography on silica gel and isolated as analytically pure colorless or slightly yellowish oils. Ligands **9a** and **9b** proved to be difficult to purify by chromatography, but according to NMR and mass spectrometry the crude products were of high purity and used as such for the preparation of the metal complexes. To study the influence of the additional stereogenic centers in the chiral bridge on

the geometry and reactivity of metal complexes derived from ligands of type **10**, the (*S*,*R*,*R*,*S*)- and (*R*,*R*,*R*,*R*)-diastereomers of ligand **10a** were prepared from (*R*)- and (*S*)-chloromethyloxazoline **6a** and commercially available (*R*,*R*)-*N*,*N*′-dimethylcyclohexane-1,2-diamine.

Complexation of ligands **9a**,**b** and **10a**,**b** with anhydrous salts (MCl_2; M = Fe, Mn, Zn) in acetonitrile at room temperature under N_2 proceeded smoothly to give colorless or slightly yellow solutions of the desired metal complexes. After removal of the solvent and washing with diethyl ether, complexes **11a**,**b**–**13a**,**b** (Scheme 3) and **17a**,**b**–**19a**,**b** and **20**–**22** (Scheme 4) were isolated in high yields (70 to 90%) as microcrystalline solids, which were characterized by mass spectroscopy (FAB or ESI) and elemental analysis. Moreover, crystallization from acetonitrile or acetonitrile/diethyl ether solutions provided crystals suitable for X-ray analysis for several complexes.

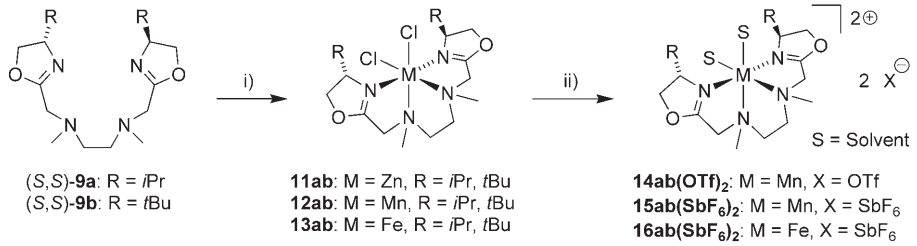

(*S*,*S*)-**9a**: R = *i*Pr
(*S*,*S*)-**9b**: R = *t*Bu

11ab: M = Zn, R = *i*Pr, *t*Bu
12ab: M = Mn, R = *i*Pr, *t*Bu
13ab: M = Fe, R = *i*Pr, *t*Bu

14ab(OTf)$_2$: M = Mn, X = OTf
15ab(SbF$_6$)$_2$: M = Mn, X = SbF_6
16ab(SbF$_6$)$_2$: M = Fe, X = SbF_6

Scheme 3. Preparation of metal complexes derived from ligands **9a** and **9b**. i) Anhydrous MCl_2, CH_3CN; ii) 2 equiv of silver salt, CH_3CN.

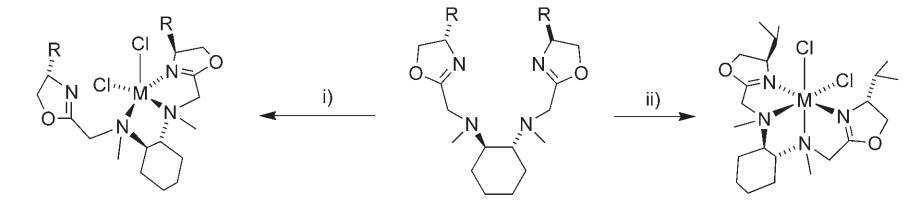

(*S*,*R*,*R*,*S*)-**17ab**: M = Zn, R = *i*Pr, *t*Bu
(*S*,*R*,*R*,*S*)-**18ab**: M = Mn, R = *i*Pr, *t*Bu
(*S*,*R*,*R*,*S*)-**19ab**: M = Fe, R = *i*Pr, *t*Bu

(*S*,*R*,*R*,*S*)-**10a**: R = *i*Pr
(*R*,*R*,*R*,*R*)-**10a**: R = *i*Pr
(*S*,*R*,*R*,*S*)-**10b**: R = *t*Bu

(*R*,*R*,*R*,*R*)-**20**: M = Zn
(*R*,*R*,*R*,*R*)-**21**: M = Mn
(*R*,*R*,*R*,*R*)-**22**: M = Fe

Scheme 4. Preparation of metal complexes derived from ligands **10a** and **10b**. i) Anhydrous MCl_2, (*S*,*R*,*R*,*S*)-**10a**,**b**, CH_3CN, RT; ii) anhydrous MCl_2, (*R*,*R*,*R*,*R*)-**10**, CH_3CN, RT.

For catalytic studies, we also prepared ionic versions of the Fe and Mn complexes with weakly coordinating anions to generate two vacant coordination sites (Scheme 3). Starting from the dichloro complexes, the chloride anions were removed by precipitation as AgCl to give the corresponding trifluoromethanesulfonate (OTf^-), hexafluoroantimonate, or hexafluorophosphate complexes. All complexes were characterized by elemental analysis and mass spectroscopy (FAB or ESI). The mass spectra of the hexafluoroantimonate or hexafluorophosphate salts generally showed a main signal corresponding to a monofluoro complex $[(L)M(F)]^+$ (L = ligand; M = Mn, Fe). The abstraction of fluoride from SbF_6^- or PF_6^- most likely occurs in the mass spectrometer, as elemental analyses and crystal structures were consistent with the general formula $[(L)M][X]_2$ (X = SbF_6 or PF_6).[20]

Structural characterization of metal complexes: The Zn^{II} complexes **11a** and **11b** were prepared for NMR studies, as they were expected to be isostructural to the corresponding paramagnetic $FeCl_2$ and $MnCl_2$ complexes. The ^1H NMR spectra of the diamagnetic zinc complexes in CD_2Cl_2 were consistent with a C_2 symmetric structure with a single set of signals for the *i*Pr (**11a**) and *t*Bu (**11b**) substituents, respectively, and also only one signal for the methylamino groups. Notably, the ethylene protons, which appear as singlet-like signals in the NMR spectra of the free ligands, now give rise to pairs of doublets, as a consequence of the more rigid structure of the metal complexes, in which the diastereotopic protons experience distinctly different environments. Analysis of the NMR and MS data clearly confirms the structural formulas of complexes **11a** and **11b**.

The flexible tetradentate ligand can adopt different conformations when coordinating to a metal center (Figure 2) and form three diastereomeric complexes (*trans*, *cis*-α and *cis*-β). In order to establish the coordination mode in complexes **12a** and **13a** by means of X-ray analysis, the compounds were recrystallized from a mixture of acetonitrile and diethyl ether, to yield colorless and pale green crystals, respectively, which were used for crystal structure determination.

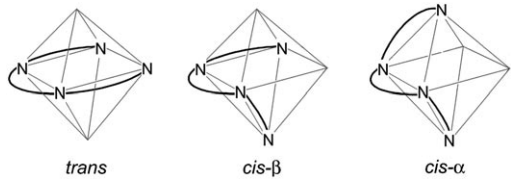

Figure 2. Stereoisomers of octahedral metal complexes.

As expected, the Mn and Fe complexes formed analogous structures (Figure 3; crystallographic data: Table 5). Complex **13a** possesses crystallographically imposed C_2 symmetry, the twofold axis running through the metal ion and bisecting the Cl–Fe–Cl angle. The ligand is tetracoordinated to the metal center, which adopts a distorded octahedral geometry with two oxazoline N atoms in axial positions, and the two amine N atoms in equatorial positions. The remain-

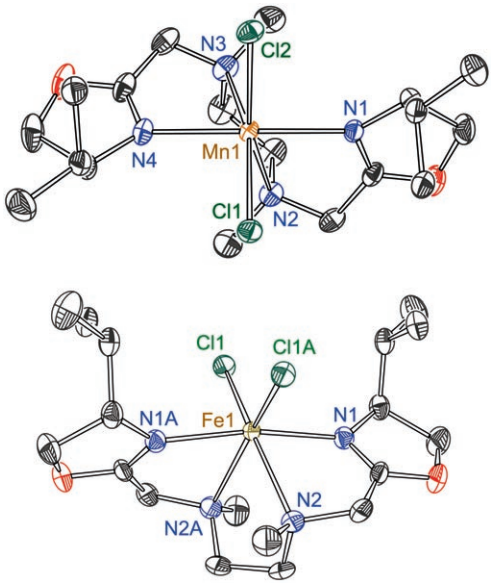

Figure 3. ORTEP drawing of Mn^{II} complex **12a** (top) and Fe^{II} complex **13a** (50% thermal ellipsoids). The hydrogen atoms have been omitted for clarity.

ing two equatorial coordination sites are occupied by the two chloride ions. This arrangement, the *cis*-α-configuration, is by far the most frequently observed coordination mode for ligands of this type.[9a,10a,21–32]

The chiral ligand can chelate the metal ion in two different ways, forming two helical diastereomers of *Δ* and *Λ* helicity. By analysis of the crystal structures, the *Δ* configuration was assigned to both the Mn and Fe complexes **12a** and **13a**. As mentioned above, the NMR spectrum of the Zn complexes **11a** and **11b** was consistent with the selective formation of only one diastereomer, this suggests that the coordination mode observed in complexes **11**–**13** is thermodynamically favored. Apparently, the stereoselectivity of complex formation is controlled by the substituents at the stereogenic centers of the oxazoline rings.

Selected structural parameters of the two structures are listed in Table 1. The bond lengths and angles in the $[MN_4Cl_2]$ core are very similar. The mean value of the metal–nitrogen distances are; 2.33 Å for the Mn and 2.26 Å for the Fe complex, and are consistent with the presence of high-spin Mn^{II} and Fe^{II} atoms. This is in agreement with the NMR spectrum of iron complex **13a** in CD_3CN. As expected, the metal bonds to the oxazoline N atoms are shorter than those to the amino groups, as a consequence of the sp^2-hybridization of the oxazoline N atom and the metal-oxazoline π interaction. An edge-on perspective of the two complexes shows a severe distortion from a pseudo-square planar arrangement, defined by two amine N atoms and the two chloride atoms. Deviations from the least-squares mean plane are indicative of this distortion (Table 2; mean deviation of 0.29 Å for **12a** and 0.27 Å for **13a**). The angles N1–M–N2 (72.3°) and N4–M–N2 (96.0°) for **12a** and N1–M–N2 (74.4°) and N1A–M–N2 (97.9°) for **13a**, are also characteristic of the distorted octahedral geometry. This deformation most likely results from geometrical constraints imposed by the two oxazoline rings and the presence of five-membered metallacycles, which enforce an angle around the metal atom close to 75°. An additional characteristic of the two complexes is the rather large Cl–M–Cl angle of 113.7° and 112.6° in **12a** and **13a**, respectively.

Crystals of **16b(PF$_6$)$_2$**, the ionic analogue of **13b**, that were suitable for X-ray analysis, were obtained in acetonitrile/diethylether (see Figure 4; crystallographic data: Table 5). The conformation of the ligand and the pseudo-octahedral coordination geometry are quite similar in the dichloro and the ionic complex, although some deviations of

Table 1. Selected bond lengths [Å] and angles [°] for complexes **12a**, **13a** and **16b(PF$_6$)$_2$**.

Complex **12a**			
Mn1–Cl1	2.4231(5)	N1–Mn1–N2	72.22(5)
Mn1–Cl2	2.4272(5)	N3–Mn1–N4	72.49(5)
Mn1–N1	2.2413(14)	N2–Mn1–N3	74.81(5)
Mn1–N4	2.2599(14)	N1–Mn1–N3	96.11(5)
Mn1–N2	2.4304(13)	N2–Mn1–N4	95.97(5)
Mn1–N3	2.4030(13)	Cl1–Mn1–Cl2	113.684(16)
		N1–Mn1–N4	165.68(4)
Complex **13a**			
Fe1–Cl1	2.3917(5)	N1–Fe1–N2	74.43(6)
Fe1–Cl1A[a]	2.3917(5)	N2A–Fe1–N1A	74.43(6)
Fe1–N1	2.1816(17)	N2–Fe1–N2A	77.19(9)
Fe1–N1A	2.1816(17)	N1–Fe1–N2A	97.85(6)
Fe1–N2	2.3383(18)	N2–Fe1–N1A	97.85(6)
Fe1–N2A	2.3383(18)	Cl1–Fe1–Cl1A	112.61(3)
		N1–Fe1–N1A	170.33(9)
Complex **16b(PF$_6$)$_2$**			
Fe1–N5	2.1404(18)	N1–Fe1–N2	78.19(6)
Fe1–N6	2.1466(18)	N3–Fe1–N4	78.23(6)
Fe1–N1	2.1608(15)	N2–Fe1–N3	80.56(6)
Fe1–N4	2.1748(15)	N1–Fe1–N3	90.15(6)
Fe1–N2	2.2909(18)	N2–Fe1–N4	91.60(6)
Fe1–N3	2.2931(17)	N5–Fe1–N6	93.74(6)
		N1–Fe1–N4	165.73(6)

[a] The symmetry operator to generate the positions of Cl1A and N2A is $x, -y, -z$.

Table 2. Deviation [Å] of atoms from the calculated equatorial least-squares mean plane[a] for complexes **12a**, **13a**, **16b(PF$_6$)$_2$** and **18b**.

	12a	**13a**	**16b(PF$_6$)$_2$**	**18b**
Cl1	0.2404(4)	0.2297(5)	–	–
Cl1A	–	–0.2297(5)	–	–
Cl2	–0.2411(4)	–	–	0.1409(4)
N1	–	–	–	–0.1798(12)
N2	–0.3395(14)	–0.3190(18)	–0.1426(18)	0.2092(13)
N2A	–	0.3190(18)	–	–
N3	0.3402(14)	–	0.1424(18)	–0.1703(13)
N5	–	–	0.135(2)	–
N6	–	–	–0.1348(18)	–
M	0.0076(3)	0.0000	0.0287(3)	0.6472(2)

[a] Atoms used to calculate the least-squares mean plane are as follows: Cl1, Cl2, N2, N3 for **12a**; Cl1, N2, Cl1A, N2A for **13a**; N2, N3, N5, N6 for **16b(PF$_6$)$_2$**; Cl2, N1, N2, N3 for **18b**.

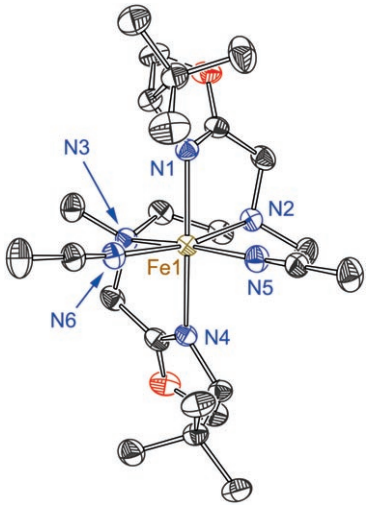

Figure 4. ORTEP drawing of Fe^{II} complex **16b(PF$_6$)$_2$** (50% thermal ellipsoids). The hydrogen atoms and the counterions have been omitted for clarity.

the metal–nitrogen distances and angles are observed. The two vacant sites generated by abstraction of the two chloride ions are occupied by two molecules of acetonitrile, while the hexafluorophosphate counteranions are located at the periphery and do not interact with the metal ion. The N_6 pseudo-octahedral core is less distorted than in the dichloro complex, as revealed by the deviations from the least-square mean plane defined by N2, N3, N5, and N6 (0.14 Å; see Table 2). The N–Fe–N angles in the five-membered chelate rings, namely N1–Fe–N2 (78.2°), N3–Fe–N4 (78.2°) and N2–Fe–N3 (80.6°) are still smaller than the ideal 90°, but to a lesser extent than in the case of the dichloro complex **13a**. Furthermore, the N1–Fe–N3 and N2–Fe–N4 angles are both close to 90° (90.2° and 91.6°, respectively), and the N5–Fe–N6 angle is also distinctly smaller than the Cl–Fe–Cl angle in **13a** (93.7° vs. 112.6°). As expected, the metal–amine bonds in the ionic complex are ≈0.05 Å shorter than in the neutral complex **13a**. Although there is no crystallographically imposed C_2 symmetry, the symmetry of the ligand is largely retained, with a pseudo axis across the Fe atom and the center of the diamine bridge.

Ligands **10a** and **10b** showed a distinctly different coordination behavior than their analogues **9a** and **9b**. Depending on whether the (*S*,*R*,*R*,*S*)- or (*R*,*R*,*R*,*R*)-isomer was used, different coordination modes were observed upon complexation with $ZnCl_2$, $FeCl_2$, or $MnCl_2$ (Scheme 4).

The ^{1}H and ^{13}C NMR spectra of the Zn complexes (*S*,*R*,*R*,*S*)-**17a** and (*S*,*R*,*R*,*S*)-**17b** showed two distinct sets of signals for the oxazoline moities as well as for the methylamino groups. This implies that the C_2-symmetry of the ligand was lost in the complex. Studies of the 2-D NMR spectra indicated a *cis*-β configuration for the complex with a *cis* arrangement of the two oxazoline rings. A preference for this coordination mode over the *cis*-α configuration has been reported for metal complexes of similar tetradentate ligands such as a 6-methylpyridine derivative of a bpmcn complex (Figure 1), namely [Fe(6-Me$_2$-bpmcn)(CF$_3$SO$_3$)$_2$].[33]

Crystals suitable for X-ray analysis were obtained for the manganese derivative (*S*,*R*,*R*,*S*)-**18b** by means of crystallization from acetonitrile (Figure 5; crystallographic data: Table 5). The general structural features of the complexed ligand are consistent with the NMR spectra of (*S*,*R*,*R*,*S*)-**17b**, but, notably, the metal center is only pentacoordinated, since one oxazoline ring is positioned too distant from the Mn atom to form a bond (Mn–N4 = 3.39 Å). The coordination geometry of (*S*,*R*,*R*,*S*)-**18b** can be described as a distorted square pyramidal structure ($\tau = 0.45$)[34] with the apical position occupied by one chloride, Cl1, and the distorted square formed by the second chloride atom Cl2, the two tertiary amino groups, N2 and N3, and the oxazoline N1 atom. The deviation of the Mn atom from the calculated least square plane is 0.6472(2) Å (Table 2; for main structural parameters: see Table 3).

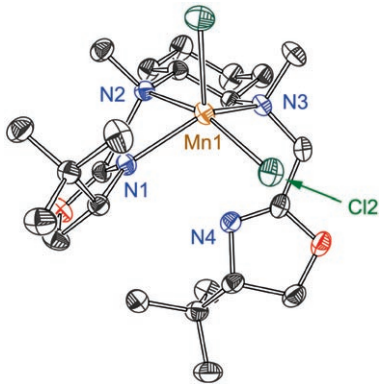

Figure 5. ORTEP drawing of Mn^{II} complex **18b** (50% thermal ellipsoids). The hydrogen atoms have been omitted for clarity.

The remarkably different behavior of the diastereomeric ligand, (*R*,*R*,*R*,*R*)-**10a**, is illustrated by the Zn complex (*R*,*R*,*R*,*R*)-**20**. The NMR spectra in CD_2Cl_2 and [D$_8$]THF were consistent with a C_2-symmetric structure. At ambient temperature some signal broadening was observed, but at −18 °C in [D$_8$]THF, a well resolved spectrum was obtained, with sharp signals that could be fully assigned (see the Experimental Section). Colorless crystals of (*R*,*R*,*R*,*R*)-**20** suitable for X-ray analysis were grown from a concentrated solution in acetonitrile at room temperature (Figure 6; crystallographic data: Table 5; selected bond lengths and angles: Table 3). The three-dimensional arrangement of the ligand backbone and the oxazoline moieties in this complex closely resembles that found in Fe and Mn complexes **12a** and **13a** (Figure 3). As expected from the *R* configuration of the oxazoline rings, the ligand forms a Λ-helix, confirming that steric effects of the oxazoline substituents determine the helical chirality.

Crystals of the cationic bis-acetonitrile Mn complex **21-(SbF$_6$)$_2$** were grown by slow diffusion of diethylether into a

Table 3. Selected bond lengths [Å] and angles [°] for complexes **18b**, **20** and **21(SbF$_6$)$_2$**.

Complex **18b**			
Mn1–Cl1	2.3822(5)	N1–Mn1–N2	73.55(5)
Mn1–Cl2	2.4003(5)	N1–Mn1–Cl1	113.93(4)
Mn1–N1	2.1926(13)	N2–Mn1–N3	75.18(5)
Mn1–N2	2.3974(14)	Cl2–Mn1–N2	157.27(3)
Mn1–N3	2.3170(14)	N2–Mn1–Cl1	94.04(3)
Mn1–N4	3.3924(14)	N3–Mn1–Cl1	105.71(4)
		N1–Mn1–N3	130.42(5)
		Cl1–Mn1–Cl2	108.552(19)
Complex **20**			
Zn1–Cl1	2.3316(7)	N1–Zn1–N2	74.67(8)
Zn1–Cl2	2.3764(7)	N3–Zn1–N4	73.07(9)
Zn1–N1	2.211(2)	N2–Zn1–N3	75.29(8)
Zn1–N4	2.231(2)	N1–Zn1–N3	92.92(8)
Zn1–N2	2.331(2)	N2–Zn1–N4	92.33(8)
Zn1–N3	2.356(2)	Cl1–Zn1–Cl2	104.09(3)
		N1–Zn1–N4	163.12(8)
Complex **21(SbF$_6$)$_2$**			
	A	B	A	B
Mn1–N5	2.220(5)	2.281(4)	N1–Mn1–N2	75.54(13)	76.36(13)
Mn1–N6	2.248(4)	2.233(4)	N3–Mn1–N4	75.83(13)	75.55(13)
Mn1–N1	2.215(4)	2.188(4)	N2–Mn1–N3	78.98(12)	77.97(12)
Mn1–N4	2.199(4)	2.204(3)	N1–Mn1–N3	98.08(13)	99.28(13)
Mn1–N2	2.311(3)	2.301(3)	N2–Mn1–N4	99.03(13)	98.25(13)
Mn1–N3	2.289(3)	2.305(4)	N5–Mn1–N6	87.83(17)	88.64(17)
			N1–Mn1–N4	172.66(13)	173.34(14)

saturated acetonitrile solution. The solid-state structure of this complex, determined by X-ray diffraction, is very similar to the structure of the dichloro-Zn complex, as shown in Figure 6 (crystallographic data: Table 5; selected bond lengths and angles: Table 3).

The remarkably different coordination chemistry of the (*S*,*R*,*R*,*S*)- and (*R*,*R*,*R*,*R*)-diastereomers of ligand **10** may be attributed to the rigid conformation imposed by the *trans*-diaminocyclohexane unit. While the *R*,*R*,*R*,*R* configuration allows the formation of C_2-symmetric tetracoordinated complexes with a *cis*-α configuration, which is also favored by the more flexible ligand **9**, the *S*,*R*,*R*,*S* configuration prevents this coordination mode and impedes the coordination of both oxazoline rings.

Catalysis: Stack et al. have shown that manganese complexes derived from (*R*,*R*)-bpmcn are efficient catalysts for the epoxidation of a wide range of olefins by using peracetic acid as oxidant.[9] Therefore, we decided to test our manganese complexes prepared from ligands **9a**,**b** and **10a**,**b** as catalysts for analogous enantioselective epoxidations. In a typical run, 1.5 equivalents of 32% aqueous peracetic acid solution were slowly added to a mixture of 1.0 equivalent of alkene and 5 mol% of catalyst in acetonitrile at −30 °C.

Using cationic complexes **14a** and **14b**, almost complete conversion of vinyl-cyclohexane, indene or *trans*-β-methylstyrene was observed after 30 min and epoxides were obtained in yields of up to 94% (97% for indene). However, no asymmetric induction was achieved (<6% *ee* in all cases). Surprisingly, when the dichloro complexes **12a** and **12b** were used, the same conversions and yields were obtained.

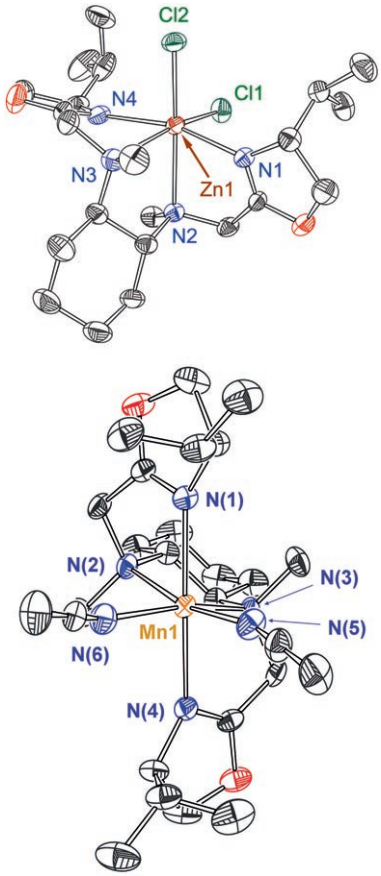

Figure 6. ORTEP drawing of Zn^{II} complex **20** (top) and Mn^{II} complex **21-(SbF$_6$)$_2$** (50% thermal ellipsoids). The hydrogen atoms and the counterions have been omitted for clarity.

We next tested complexes derived from ligands **10a**,**b**, which we expected to behave differently, based on their coordination chemistry discussed above. We hoped that the conformationally more rigid *trans*-diaminocyclohexane bridge would enhance the kinetic and thermodynamic stability of the complexes and prevent degradation during epoxidation.[9a] In addition, we were interested to see if the different coordination modes of the two diastereomeric ligands (*R*,*R*,*R*,*R*)-**10** and (*S*,*R*,*R*,*S*)-**10** had an effect on the catalytic

Table 4. Epoxidation studies with Mn^{II} catalysts.

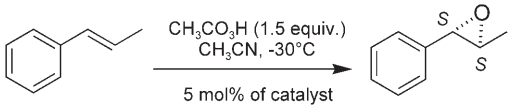

Catalyst	Conversion [%]	Yield[a] [%]	*ee* [%]
(*R*,*R*,*R*,*R*)-**21(Cl)$_2$**	<10	–	–
(*R*,*R*,*R*,*R*)-**21(OTf)$_2$**	20	86	<6
(*S*,*R*,*R*,*S*)-**18a(Cl)$_2$**	<4	–	–
(*S*,*R*,*R*,*S*)-**18a(OTf)$_2$**	38	96	18
(*S*,*R*,*R*,*S*)-**18a(SbF$_6$)$_2$**	99	97	21

[a] Based on conversion.

Table 5. Crystallographic data of complexes **12a**, **13a**, **16b(PF$_6$)$_2$**, **18b**, **20** and **21(SbF$_6$)$_2$**.

Complex	**12a**	**13a**	**16b(PF$_6$)$_2$**	**18b**	**20**	**21(SbF$_6$)$_2$**
formula	$C_{18}H_{34}Cl_2Mn_1N_4O_2$	$C_{18}H_{34}Cl_2Fe_1N_4O_2$	$C_{50}H_{91}F_{24}Fe_2N_{13}O_4P_4$	$C_{24}H_{44}Cl_2Mn_1N_4O_2$	$C_{22}H_{40}Cl_2N_4O_2Zn_1$	$C_{26}H_{46}F_{12}Mn_1N_6O_2Sb_2$
M_r	464.33	465.25	1629.9	546.47	528.87	1001.09
Z	4	2	2	4	4	4
ρ_{calc} [g cm^{-3}]	1.375	1.402	1.504	1.300	1.380	1.764
F(000)	980	492	1686	1164	1120	1980
description	pale pink block	pale green plate	purple plate	pale red block	colorless plate	pink block
crystal size [mm^3]	0.22×0.24×0.27	0.04×0.20×0.20	0.23×0.26×0.36	0.22×0.24×0.25	0.10×0.12×0.31	0.30×0.30×0.32
crystal system	orthorhombic	orthorhombic	orthorhombic	orthorhombic	orthorhombic	monoclinic
space group	$P2_12_12_1$	$P22_12_1$	$P22_12_1$	$P2_12_12_1$	$P2_12_12_1$	$P2_1$
a [Å]	9.0262(8)	7.5728(7)	10.6449(1)	9.9811(2)	9.0648(1)	9.0474(2)
b [Å]	15.2617(15)	8.9244(4)	14.9076(1)	13.9113(3)	12.2302(1)	35.9055(8)
c [Å]	16.2781(9)	16.3012(15)	22.6736(2)	20.1114(4)	22.9624(3)	11.7475(2)
α [°]	90	90	90	90	90	90
β [°]	90	90	90	90	90	99.0743(6)
γ [°]	90	90	90	90	90	90
V [Å^3]	2242.4(3)	1101.68(15)	3598.07(5)	2792.47(10)	2545.71(5)	3768.43(13)
λ [Å]	0.71073	0.71073	0.71073	0.71073	0.71073	0.71073
T [°C]	173	173	173	173	173	173
μ [mm^{-1}]	0.847	0.947	0.604	0.691	1.200	1.846
min/max transmission	0.82/0.83	0.83/0.96	0.85/0.87	0.85/0.86	0.87/0.89	0.57/0.57
θ range [°]	3.37–32.502	3.385–31.994	1.635–27.835	1.780–30.079	1.774–27.899	1.134–27.489
N collected[a]	93522	30061	31475	25975	21500	28237
N independent[b]	8089 (merging r=0.039)	3822 (merging r=0.066)	8542 (merging r=0.084)	8177 (merging r=0.057)	6069 (merging r=0.074)	16981 (merging r=0.043)
N observed[c]	4490	1953	5750	6416	5068	13684
N parameters[d]	245	192	494	299	281	884
R[e]	0.0205	0.0234	0.0259	0.0287	0.0339	0.0309
wR_2	0.0357	0.0256	0.0398	0.0386	0.0427	0.0430
GOF	1.0713	1.0793	1.0740	1.0952	0.9209	1.1212

[a] N collected is the number of reflections collected. [b] N independent is the number of independent reflections. [c] N observed is the total number of the independent reflections having $I>3.00\sigma(I)$. [d] Number of parameters that have been refined using the reflections considered as observed. [e] Calculated on the reflections considered as observed.

properties. With the C_2-symmetric tetracoordinated ionic complex **21(OTf)$_2$**, no enantiomeric excess and low conversion was observed (Table 4). The dichloro complex **21(Cl)$_2$** was even less active (<10% conv), in contrast to the analogous complexes **12a** and **12b**, based on diaminoethane-derived ligands. The different activities of **12a**,**b** and **21** may be the result of the stabilizing effect of the diaminocyclohexane unit,[9a] which prevents dissociation of a chloride from the inactive dichloro complex **21(Cl)$_2$**, whereas in the more labile complexes **12a** and **12b** partial dissociation of one or more M–N bonds generates vacant sites that are necessary for catalytic activity.

Manganese complexes **18a**,**b(Cl)$_2$** derived from the diastereomeric ligands (*S*,*R*,*R*,*S*)-**10a**,**b** also showed no catalytic activity, whereas the corresponding trifluoromethanesulfonate **18a(OTf)$_2$** gave moderate conversion and the hexafluoroantimonate **18a(SbF$_6$)$_2$** full conversion. The trifluoromethanesulfonate and hexafluoroantimonate salts both induced modest, but reproducible enantiomeric excesses of ≈20%, which, notably, remained constant during the course of the reaction.

We also carried out preliminary catalytic studies with iron complexes. However, all complexes were found to be less active and less enantioselective (up to 12% *ee*) than analogous manganese-based catalysts.

Conclusion

Two classes of readily accessible modular chiral diamino–bisoxazoline ligands have been prepared and converted to a series of Fe^{II}, Mn^{II}, and Zn^{II} complexes. The coordination chemistry of these ligands strongly depends on the backbone. Bisoxazolines containing a diaminoethane bridge act as tetradentate ligands and selectively form metal complexes [MN$_4$L$_2$] with *cis*-α configuration of the [MN$_4$] core. The same behavior is observed for ligands assembled from two (*R*)-oxazolines and (*R*,*R*)-1,2-diaminocyclohexane, whereas the corresponding diastereomeric (*S*,*R*,*R*,*S*)-ligands prefer a different coordination mode, leading to pentacoordinated [MN$_3$L$_2$] complexes with only one coordinated oxazoline ring. The pentacoordinated manganese complexes with weakly coordinating anions proved to be active catalysts for the epoxidation of olefins with peracetic acid. Although the enantioselectivities were modest, the modular structure of the ligands, which can be easily modified, should leave room for improvement. Moreover, ligands of this type may prove useful for other applications in asymmetric catalysis.

Experimental Section

General: All chemicals were purchased from commercial sources and used as received, unless noted otherwise. Anhydrous solvents were obtained in sure-seal bottles from Fluka or purified using standard methods.[35] All reactions were carried out in an atmosphere of purified nitrogen by using a glovebox and standard Schlenk techniques.

NMR: Bruker Advance DRX 500 (^{1}H: 500 MHz, ^{13}C: 125.8 MHz), Bruker AMX 400 (^{1}H: 400 MHz, ^{13}C: 100.6 MHz) or Bruker AC 250. Chemical shifts (δ are listed relative to tetramethylsilane as an internal standard; ox = oxazoline).

Mass spectrometry: Finnegan MAT 312 (FAB), VG 70-SE (70 eV) (EI) in *m*/*z* (% of base peak).

Optical rotation: Perkin–Elmer 341 polarimeter (sodium lamp, 1-dm cuvette, *c* in g/100 mL, 20 °C).

Gas chromatography: Carlo Erba HRGC Mega2 series MFC 800.

Elemental analyses: were performed by the Microanalytical Laboratory of the Department of Chemistry, University of Basel.

Compounds **3**,[18] **5**[36] and **6**[18] were prepared following published procedures.

Synthesis of (4*R*)-2-chloromethyl-4-isopropyl-4,5-dihydrooxazole ((*R*)-6a)—procedure starting from chloroacetamide: Burgess reagent (methyl-*N*-triethylammoniosulfonylcarbamate; 3.78 g, 15.86 mmol) was added to a solution of amide (*R*)-**3a** (2.77 g, 15.42 mmol) in THF (30 mL) at room temperature. After refluxing the reaction mixture for 5 h, the volatiles were evaporated and the residue was dissolved in CH_2Cl_2 (20 mL). The solution was washed with water (2×20 mL). After separation of the organic phase, the aqueous layer was extracted twice with CH_2Cl_2. The combined organic layers were dried over $MgSO_4$ and concentrated to give a yellowish oil, from which analytically pure (*R*)-**6a** was obtained by distillation (b.p. 42 °C, 0.04 mbar) as a colorless oil (1.55 g, 62 %).

Synthesis of (*R*)-6a—procedure starting from methyl chloroacetimidate hydrochloride (5): Methyl chloroacetimidate hydrochloride (1.72 g, 11.9 mmol) and D-valinol (1.23 g, 11.9 mmol) were mixed in CH_2Cl_2 (40 mL), and the resulting suspension stirred at room temperature for 4 h. The solid was filtered off and the volatiles removed in vacuo to give a yellowish oil, from which analytically pure (*R*)-**6a** was obtained by distillation (b.p. 42 °C, 0.04 mbar) as a colorless oil (1.1 g, 57 %). $[\alpha]_D$ = +99.2 (*c* = 1.19 in $CHCl_3$); ^{1}H NMR (500 MHz, $CDCl_3$, 25 °C): δ = 4.33 (m, 1H; OC*H*H), 4.09 (m, 2H; $ClCH_2$), 4.04 (m, 1H; OC*H*H), 3.95 (m, 1H; NCH(*i*Pr)), 1.76 (m, 1H; C*H*(CH_3)$_2$), 0.95 (d, ^3J(H,H) = 7 Hz, 3H; CH(CH_3)$_2$), 0.87 ppm (d, ^3J(H,H) = 7 Hz, 3H; CH(CH_3)$_2$); ^{13}C NMR (125 MHz, $CDCl_3$, 25 °C, TMS): δ = 162.3 (C=N(Ox)), 72.42 (NCH(*i*Pr)), 71.18 (CH_2O), 36.44 ($ClCH_2$), 32.46 (*C*H(CH_3)$_2$), 18.66 (CH(*C*H$_3$)$_2$), 18.07 ppm (CH(CH_3)$_2$); MS(FAB): *m*/*z* (%): 162 (100) $[M+H]^+$; elemental analysis calcd (%) for $C_7H_{12}ClNO$ (161.6): C 52.02, H 7.48, N 8.67; found: C 51.86, H 7.38, N 8.67.

General procedure for the synthesis of ligands 9: *N*,*N*′-Dimethylethylene-1,2-diamine (**7**) and K_2CO_3 were added to a solution of chloromethyloxazoline **6** in CH_3CN at room temperature, and the reaction mixture refluxed for 3 h. The solid was filtered off and volatiles removed in vacuo. EtOAc was added and the resulting colorless precipitate filtered off again. Removal of the solvents gave a yellowish oil which was used for the preparation of metal complexes without further purification. Elemental analyses were unsatisfactory and difficulties were encountered in purifying **9a** and **9b** by chromatography; however, according to NMR analyses the products were pure.

Compound ***9a***: Compound **7** (597 mg, 6.77 mmol), K_2CO_3 (4.12 g, 29.8 mmol), (*S*)-**6a** (2.21 g, 13.7 mmol), CH_3CN (16 mL), yield: 1.78 g (78 %). $[\alpha]_D$ = −82.7 (*c* = 1.2 in $CHCl_3$); ^{1}H NMR (400 MHz, $CDCl_3$, 25 °C): δ = 4.24 (m, 2H; OC*H*H), 3.95 (m, 2H; OCH*H*), 3.90 (m, 2H; NCH(*i*Pr)), 3.30 (m, 4H; CH_2), 2.64 (m, 4H; NCH_2CH_2N), 2.35 (s, 6H; NC*H*$_3$), 1.74 (m, 2H; C*H*(CH_3)$_2$), 0.95 (d, ^3J(H,H) = 6.8 Hz, 6H; CH(C*H*$_3$)$_2$), 0.87 ppm (d, ^3J(H,H) = 6.8 Hz, 6H; CH(C*H*$_3$)$_2$); ^{13}C NMR (100 MHz, $CDCl_3$, 25 °C): δ = 164.5 (C=N(Ox)), 72.2 (CH(Ox)), 70.1 (CH_2(Ox)), 54.9 (NCH_2CH_2N), 54.4 (NCH_2), 42.9 (NCH_3), 32.6 (*C*H(CH_3)$_2$), 19.0 (CH(*C*H$_3$)$_2$), 18.4 ppm (CH(*C*H$_3$)$_2$); MS(FAB): *m*/*z* (%): 339 (100) $[M+H]^+$.

Compound ***9b***: Compound **7** (420 mg, 4.76 mmol), K_2CO_3 (2.66 g, 19.2 mmol), (*S*)-**6b** (1.69 g, 9.62 mmol), CH_3CN (12 mL), yield: 1.31 g (75 %). $[\alpha]_D$ = −73.5 (*c* = 1.2 in $CHCl_3$); ^{1}H NMR (500 MHz, $CDCl_3$, 25 °C): δ = 4.17 (m, 2H; OC*H*H), 4.02 (m, 2H; OC*H*H), 3.84 (m, 2H; NCH(*t*Bu)), 3.28 (m, 4H; CH_2), 2.62 (m, 4H; NCH_2), 2.33 (s, 6H; NCH_3), 0.87 ppm (s, 18H; C(CH_3)$_3$); ^{13}C NMR (125 MHz, $CDCl_3$, 25 °C): δ = 164.4 (C=N(Ox)), 75.7 (CH(Ox)), 68.5 (CH_2(Ox)), 54.8 (NCH_2CH_2N), 54.3 (NCH_2), 42.7 (NCH_3), 33.4 (*C*(CH_3)$_3$), 25.9 ppm (C(*C*H$_3$)$_3$); MS(FAB): *m*/*z* (%): 367 (100) $[M+H]^+$.

General procedure for the synthesis of ligands 10: (*R*,*R*)-*N*,*N*′-dimethylcyclohexane-1,2-diamine (**8**) and K_2CO_3 were added to a solution of the chloromethyloxazoline **6** in CH_3CN at room temperature. The resulting reaction mixture was refluxed for 3 h. The solid was filtered off and volatiles removed in vacuo. Acetone was added and the resulting colorless precipitate filtered off again. Removal of acetone gave a yellow oil, which was purified by flash chromatography (silica gel, EtOAc, 3 vol % NEt_3).

Compound (S,R,R,S)-***10a***: Compound **8** (440 mg, 3.09 mmol), K_2CO_3 (1.72 g, 12.44 mmol), (*S*)-**6a** (1.00 g, 6.19 mmol), CH_3CN (10 mL), yield: 0.56 g (46 %). R_f = 0.29 (EtOAc, 3 vol % NEt_3); $[\alpha]_D$ = −78.0 (*c* = 0.98 in CH_2Cl_2); ^{1}H NMR (500 MHz, $CDCl_3$, 25 °C): δ = 4.24 (m, 2H; OC*H*H), 3.95 (m, 2H; OC*H*H), 3.89 (m, 2H; NCH(*i*Pr)), 3.49 (bd, ^2J(H,H) = 14.2 Hz, 2H; CH_2), 3.42 (bd, ^2J(H,H) = 14.2 Hz, 2H; CH_2), 2.56 (bm, 2H; NC*H*CH_2), 2.38 (m, 6H; NCH_3), 1.81 (m, 2H; NCHC*H*$_2$CH$_2$), 1.75 (m, 2H; C*H*(CH_3)$_2$), 1.68 (m, 2H; NCHCH$_2$C*H*$_2$), 1.20 (m, 2H; NCHC*H*$_2$CH$_2$), 1.08 (m, 2H; NCHCH$_2$C*H*$_2$), 0.94 (d, ^3J(H,H) = 6.8 Hz, 6H; CH(C*H*$_3$)$_2$), 0.87 ppm (d, ^3J(H,H) = 6.8 Hz, 6H; CH(C*H*$_3$)$_2$); ^{13}C NMR (125 MHz, $CDCl_3$, 25 °C): δ = 166.1 (C=N(Ox)), 72.1 (CH(Ox)), 70.0 (CH_2(Ox)), 63.6 (N*C*HCH$_2$), 52.0 (NCH_2), 37.2 (NCH_3), 32.6 (*C*H(CH_3)$_2$), 27.7 (NCH*C*H$_2$CH$_2$), 25.7 (NCHCH$_2$*C*H$_2$), 19.0 (CH(*C*H$_3$)$_2$), 18.3 ppm (CH(*C*H$_3$)$_2$); MS(FAB): *m*/*z* (%): 393 (100) $[M+H]^+$; elemental analysis calcd (%) for $C_{22}H_{40}N_4O_2$ (392.58): C 67.31, H 10.27, N 14.27; found: C 66.27, H 10.51, N 14.12.

Compound (R,R,R,R)-***10a***: Compound **8** (311 mg, 2.19 mmol), K_2CO_3 (1.21 g, 8.75 mmol), (*R*)-**6a** (0.705 g, 4.36 mmol), CH_3CN (8 mL), yield: 0.33 g (39 %). R_f = 0.29 (EtOAc, 3 vol % NEt_3); $[\alpha]_D$ = +56.6 (*c* = 0.96 in CH_2Cl_2); ^{1}H NMR (500 MHz, $CDCl_3$, 25 °C): δ = 4.23 (m, 2H; OC*H*H), 3.94 (m, 2H; OC*H*H), 3.88 (m, 2H; NCH(*i*Pr)), 3.42 (m, 4H; CH_2), 2.54 (m, 2H; NC*H*CH_2), 2.35 (m, 6H; NCH_3), 1.81 (m, 2H; NCHC*H*$_2$CH$_2$), 1.74 (m, 2H; C*H*(CH_3)$_2$), 1.66 (m, 2H; NCHCH$_2$C*H*$_2$), 1.19 (m, 2H; NCHC*H*$_2$CH$_2$), 1.07 (m, 2H; NCHCH$_2$C*H*$_2$), 0.94 (d, ^3J(H,H) = 6.8 Hz, 6H; CH(C*H*$_3$)$_2$), 0.87 (d, ^3J(H,H) = 6.8 Hz, 6H; CH(C*H*$_3$)$_2$); ^{13}C NMR (125 MHz, $CDCl_3$, 25 °C): δ = 165.9 (C=N(Ox)), 71.9 (CH(Ox)), 69.9 (CH_2(Ox)), 63.2 (N*C*HCH$_2$), 51.6 (N*C*H$_2$), 37.2 (N*C*H$_3$), 32.5 (*C*H(CH_3)$_2$), 27.1 (NCH*C*H$_2$CH$_2$), 25.6 (NCHCH$_2$*C*H$_2$), 18.8 ppm (CH(*C*H$_3$)$_2$), 18.2 (CH(*C*H$_3$)$_2$); MS(FAB): *m*/*z* (%): 393 (100) $[M+H]^+$; elemental analysis calcd (%) for $C_{22}H_{40}N_4O_2$ (392.58): C 67.31, H 10.27, N 14.27; found: C 67.08, H 10.13, N 14.35.

Compound (S,R,R,S)-***10b***: Compound **8** (704 mg, 4.95 mmol), K_2CO_3 (2.82 g, 20.4 mmol), (*S*)-**6b** (1.73 g, 9.85 mmol), CH_3CN (18 mL), yield: 1.06 g (51 %). R_f = 0.32 (EtOAc, 3 vol % NEt_3); $[\alpha]_D$ = −69 (*c* = 0.81 in CH_2Cl_2); ^{1}H NMR (500 MHz, $CDCl_3$, 25 °C): δ = 4.17 (m, 2H; OC*H*H), 4.02 (m, 2H; OC*H*H), 3.80 (m, 2H; NCH(*t*Bu)), 3.50 (d, ^2J(H,H) = 14 Hz, 2H; CH_2), 3.38 (d, ^2J(H,H) = 14 Hz, 2H; CH_2), 2.51 (m, 2H; NC*H*CH_2), 2.36 (m, 6H; NCH_3), 1.71 (m, 2H; NCHC*H*$_2$CH$_2$), 1.65 (m, 2H; NCHCH$_2$C*H*$_2$), 1.19 (m, 2H; NCHC*H*$_2$CH$_2$), 1.05 (m, 2H; NCHCH$_2$C*H*$_2$), 0.87 (s, 18H; C(C*H*$_3$)$_3$); ^{13}C NMR (125 MHz, $CDCl_3$, 25 °C): δ = 166.1 (C=N(Ox)), 75.4 (CH(Ox)), 68.6 (CH_2(Ox)), 63.2 (N*C*HCH$_2$), 52.0 (NCH_2), 36.9 (NCH_3), 33.6 (*C*(CH_3)$_3$), 27.5 (NCH*C*H$_2$CH$_2$), 26 (C(*C*H$_3$)$_3$), 25.6 ppm (NCHCH$_2$*C*H$_2$); MS(FAB): *m*/*z* (%): 421 (100) $[M+H]^+$; elemental analysis calcd (%) for $C_{24}H_{44}N_4O_2$ (420.64): C 68.53, H 10.54, N 13.32; found: C 67.93, H 10.34, N 13.16.

General procedure for the preparation of dichloro–zinc complexes: One equivalent of [$ZnCl_2$(dioxane)] was added to a solution of ligand (**9a**,**b** or **10a**,**b**) in MeCN (3 mL). The reaction mixture was stirred at room temperature for one hour. Remaining traces of solid were filtered off and

volatiles were removed in vacuo. The residue was washed with Et_2O (5 mL) and dried in vacuo to give a colorless solid which was analyzed by using NMR spectroscopy.

Complex ***11b***: [$ZnCl_2$(dioxane)] (120 mg, 0.53 mmol), (*S*,*S*)-**9b** (208 mg, 0.57 mmol), MeCN (3 mL), yield: 180 mg (67%). ^{1}H NMR (250 MHz, $CDCl_3$, 25°C): δ = 4.30 (m, 2H; OC*H*H), 4.23 (m, 2H; OC*H*H), 4.02 (m, 2H; NCH(*t*Bu)), 3.79 (d, ^2J(H,H) = 16.7 Hz, 2H; *endo*-H of NCH_2), 3.46 (d, ^2J(H,H) = 16.7 Hz, 2H; *exo*-H of NCH_2), 3.12 (d, ^2J(H,H) = 9.8 Hz, 2H; *endo*-H of NCH_2CH_2N), 2.79 (d, ^2J(H,H) = 9.8 Hz, 2H; *exo*-H of NCH_2CH_2N), 2.62 (s, 6H; NCH_3), 0.91 ppm (s, 18H; $C(CH_3)_3$); ^{13}C NMR (125 MHz, $CDCl_3$, 25°C): δ = 173 (C=N(Ox)), 73.6 (CH(Ox)), 70.6 (CH_2(Ox)), 54.0 (NCH_2CH_2N), 53.6 (NCH_2), 45.6 (NCH_3), 33.8 (*C*-$(CH_3)_3$), 25.9 ppm ($C(CH_3)_3$); MS(FAB): *m*/*z* (%): 465 (100) $[M-Cl]^+$.

Complex (S,R,R,S)-***17a***: [$ZnCl_2$(dioxane)] (136 mg, 0.606 mmol), (*S*,*R*,*R*,*S*)-**10a** (0.250 g, 0.637 mmol), MeCN (3 mL), yield: 160 mg (50%). ^{1}H NMR (500 MHz, CD_2Cl_2, 25°C): δ = 4.85 (bd, 1H; C*H*H), 4.67 (m, 1H; OC*H*H), 4.45 (m, 4H; 3H of OCH_2 and 1H from C*H*H), 4.32 (m, 1H; NCH(*i*Pr)), 4.02 (m, 1H; NCH(*i*Pr)), 3.44 (m, 1H; NC*H*CH_2CH_2), 3.13 (d, ^2J(H,H) = 15.5 Hz, 1H; C*H*H), 2.85 (d, ^2J(H,H) = 17.0 Hz, 1H; C*H*H), 2.49 (m, 1H; NC*H*CH_2CH_2), 2.45 (s, 3H; NCH_3), 2.26 (s, 3H; NCH_3), 2.13 (m, 1H; C*H*$(CH_3)_2$), 1.94–1.81 (overlapping m, 3H, NCHC*H*$_2CH_2$, C*H*$(CH_3)_2$), 1.72 (m, 1H; NCHCH$_2$C*H*H), 1.62 (m, 1H; NCHCH$_2$C*H*H), 1.45 (bm, 2H; NCHCH$_2$C*H*H overlapping with NCHC*H*HCH$_2$), 1.28 (m, 1H; NCHC*H*HCH$_2$), 1.07 (m, 1H; NCHCH$_2$C*H*H), 0.89 (d, ^3J(H,H) = 6.9 Hz, 3H; CH(C*H*$_3$)$_2$), 0.82 (d, ^3J-(H,H) = 6.9 Hz, 3H; CH(C*H*$_3$)$_2$), 0.78 ppm (2 overlapping d, ^3J(H,H) = 7 Hz, 6H; CH(C*H*$_3$)$_2$); ^{13}C NMR (125 MHz, CD_2Cl_2, 25°C): δ = 174.5 (C=N(Ox)), 172.7 (C=N(Ox)), 72.2 (CH_2(Ox)), 71.2 (CH_2(Ox)), 66.8 (NCH(*i*Pr)), 65.7 (NCH(*i*Pr)), 62.9 (NCH of cyclohexane), 62.5 (NCH of cyclohexane), 54.0 (CH_2), 49.1 (CH_2), 45.1 (NCH_3), 37.9 (NCH_3), 30.7 (*C*H$(CH_3)_2$), 30.4 (*C*H$(CH_3)_2$), 24.6 (NCHCH$_2$*C*H$_2$), 23.8 (NCH*C*H$_2$CH$_2$), 23.5 (NCHCH$_2$*C*H$_2$), 23.2 (NCH*C*H$_2$CH$_2$), 19.4 (CH(*C*H$_3$)$_2$), 18.7 (CH-(*C*H$_3$)$_2$), 14.6 (CH(*C*H$_3$)$_2$), 14.4 ppm (CH(*C*H$_3$)$_2$); MS(FAB): *m*/*z* (%): 491 (100) $[M-Cl]^+$.

Complex (S,R,R,S)-***17b***: [$ZnCl_2$(dioxane)] (77 mg, 0.343 mmol), (*S*,*R*,*R*,*S*)-**10b** (0.150 g, 0.357 mmol), MeCN (2 mL), yield: 70 mg (37%). ^{1}H NMR (500 MHz, CD_2Cl_2, 25°C): δ = 4.58 (m, 1H; OC*H*H of coordinated oxazoline [Ox^c]), 4.45 (m, 1H; OC*H*H [Ox^c]), 4.30 (d, 1H; *endo*-H of CH_2) overlapping with 4.29 (m, 1H; NCH(*t*Bu) [Ox^c]), 4.15 (m, 1H; OC*H*H of non-coordinated oxazoline [Ox^n]), 4.03 (d, 1H; C*H*H) overlapping with 4.03 (m, 1H; OC*H*H [Ox^n]), 3.61 (m, 1H; NCH(*t*Bu) [Ox^n]) overlapping with 3.60 (m, 1H; NCH of cyclohexane), 3.29 (d, ^2J(H,H) = 17.2 Hz, 1H; C*H*H), 2.85 (d, ^2J(H,H) = 16.7 Hz, 1H; *exo*-H of CH_2), 2.74 (dt, ^3J(H,H) = 3.9 Hz, ^3J(H,H) = 11.4 Hz, 1H; NCH of cyclohexane), 2.62 (s, 3H; NCH_3), 2.48 (s, 3H; NCH_3), 2.20 (m, 1H; NCHC*H*HCH$_2$), 1.97 (m, 1H; NCHC*H*HCH$_2$), 1.87 (m, 1H; NCHCH$_2$C*H*H), 1.83 (m, 1H; NCHCH$_2$C*H*H), 1.30 (m, 1H; NCHC*H*HCH$_2$), 1.21 (m, 1H; NCHCH$_2$C*H*H), 1.13 (m, 1H; NCHCH$_2$C*H*H), 1.10 (m, 1H; NCHC*H*HCH$_2$), 1.0 (s, 9H; $C(CH_3)_3$), 0.84 ppm (s, 9H; $C(CH_3)_3$); ^{13}C NMR (125 MHz, CD_2Cl_2, 25°C): δ = 173.3 (C=N [Ox^c]), 164.7 (C=N [Ox^n]), 76.9 (CH [Ox^n]), 73.8 (CH_2 [Ox^c]), 70.7 (CH [Ox^c]), 68.4 (CH_2 [Ox^n]), 63.1 (NCH of cyclohexane), 60.1 (NCH of cyclohexane), 51.7 (CH_2), 48.6 (CH_2), 45.2 (NCH_3), 41.7 (NCH_3), 34.8 (*C*$(CH_3)_3$ [Ox^c]), 34.2 (*C*$(CH_3)_3$ [Ox^n]), 26.3 (C(*C*H$_3$)$_3$ [Ox^n]), 26.2 (C(*C*H$_3$)$_3$ [Ox^c]), 25.8 (NCHCH$_2$*C*H$_2$), 25.2 (NCHCH$_2$*C*H$_2$), 24.7 (NCH*C*H$_2$CH$_2$), 23.2 ppm (NCH*C*H$_2$CH$_2$); MS(FAB): *m*/*z* (%): 519 (100) $[M-Cl]^+$.

Complex (R,R,R,R)-***20***: [$ZnCl_2$(dioxane)] (110 mg, 0.49 mmol), (*R*,*R*,*R*,*R*)-**10a** (0.204 g, 0.519 mmol), MeCN (3 mL), yield: 0.21 g (81%). ^{1}H NMR (500 MHz, [D$_8$]THF, −18°C): δ = 4.38 (dd, ^3J(H,H) = 6.2 Hz, ^3J-(H,H) = 8.6 Hz, 2H; CH(*i*Pr)), 4.33 (m, 2H; OC*H*H), 4.17 (m, 2H; OC*H*H), 3.76 (d, ^2J(H,H) = 15.4 Hz, 2H; *endo*-H of CH_2), 3.21 (d, ^2J-(H,H) = 15.4 Hz, 2H; *exo*-H of CH_2) overlapping with 3.19 (m, 2H; C*H*-$(CH_3)_2$), 2.45 (s, 6H ; NCH_3), 2.27 (m, 2H ; NC*H*CH_2), 1.94 (m, 2H; NCHC*H*HCH$_2$), 1.73 (m, 2H; NCHCH$_2$C*H*H), 1.28 (m, 2H; NCHC*H*HCH$_2$), 1.12 (m, 2H; NCHCH$_2$C*H*H), 0.90 (d, ^3J(H,H) = 6.8 Hz, 6H; CH(C*H*$_3$)$_2$), 0.78 ppm (d, ^3J(H,H) = 6.8 Hz, 6H; CH(C*H*$_3$)$_2$); elemental analysis calcd (%) for $C_{22}H_{40}N_4O_2Cl_2Zn$ (528.87): C 49.96, H 7.62, N 10.59; found: C 49.99, H 7.45, N 10.54. Crystals suitable for X-ray analysis were grown from acetonitrile at room temperature.

Preparation of dichloro manganese and iron complexes of ligands 9a,b—synthesis of 12a: A solution of (*S*,*S*)-**9a** (0.5 g, 1.477 mmol) in MeCN (5 mL) was added to a suspension of $MnCl_2$ (0.176 g, 1.399 mmol) in MeCN (5 mL) at room temperature to give, after a few minutes, a bright orange solution which was stirred for further 3 h. The volatiles were removed and the residue washed with Et_2O (10 mL) to give a colorless compound, which was dried in vacuo; yield: 0.55 g (81%) of **12a**. MS-(FAB): *m*/*z* (%): 428 (100) $[M-Cl]^+$; elemental analysis calcd (%) for $C_{18}H_{34}Cl_2MnN_4O_2$ (464.33): C 46.56, H 7.38, N 12.07; found: C 46.30, H 7.37, N 12.07. Crystals suitable for X-ray analysis were grown in MeCN/Et_2O solution at room temperature.

Complex ***13a***: $FeCl_2$ (0.176 g, 1.389 mmol), (*S*,*S*)-**9a** (0.495 g, 1.462 mmol), MeCN (10 mL), yield: 0.47 g (73%). MS(FAB): *m*/*z* (%): 429 (100) $[M-Cl]^+$; elemental analysis calcd (%) for $C_{18}H_{34}Cl_2FeN_4O_2$ (465.25): C 46.47, H 7.37, N 12.04; found: C 46.20, H 7.10, N 12.02. Crystals suitable for X-ray analysis were grown in a MeCN/Et_2O solution at room temperature.

Preparation of OTf and SbF_6 salts 14a,b–16a,b—synthesis of 15a(OTf)$_2$: AgOTf (0.16 g, 0.623 mmol) was added to a solution of **13a** (0.149 g, 0.320 mmol) in MeCN (5 mL) at room temperature. The reaction mixture was stirred for 2 d protected from light by aluminum foil. The solid was filtered off and the red-brown solution concentrated to ≈0.5 mL. Et_2O was added to precipitate a light brown solid, which was dried in vacuo to yield 190 mg (86%) of **15a(OTf)$_2$**. MS(FAB): *m*/*z* (%): 543 (100) $[M-OTf]^+$; elemental analysis calcd (%) for $C_{20}H_{34}F_6FeN_4O_8S_2$ (692.48): C 34.69, H 4.95, N 8.09; found: C 34.95, H 5.37, N 7.90.

Complex ***15a(SbF$_6$)$_2$***: $AgSbF_6$ (0.226 g, 0.658 mmol), **13a** (0.146 g, 0.314 mmol), MeCN (5 mL), yield: 220 mg (74%) of an orange solid. MS(FAB): *m*/*z* (%): 629 (28) $[M-SbF_6]^+$, 413 (100) [(**9a**)Fe(F)]$^+$; elemental analysis calcd (%) for $C_{18}H_{34}F_{12}FeN_4O_2Sb_2$·1MeCN (906.9): C 26.49, H 4.11, N 7.72; found: C 26.13, H 4.12, N 8.35.

Complex ***15b(SbF$_6$)$_2$***: $AgSbF_6$ (0.118 g, 0.343 mmol), **13b** (0.100 g, 0.203 mmol), MeCN (3 mL), yield: 123 mg (75%) of an orange solid. Elemental analysis calcd (%) for $C_{20}H_{38}F_{12}FeN_4O_2Sb_2$·1.5MeCN (955.45): C 28.91, H 4.48, N 8.06; found: C 29.14, H 4.75, N 7.78.

Fe(PF$_6$)$_2$ salt of (*S*,*S*)-9b: $TlPF_6$ (0.14 g, 0.40 mmol), **13b** (0.101 g, 0.205 mmol), MeCN (2 mL), yield: 0.12 g (74%) of a yellowish solid. MS-(FAB): *m*/*z* (%): 441 (100) [(**9b**)Fe(F)]$^+$; elemental analysis calcd (%) for $C_{22}H_{38}F_{12}FeN_4O_2P_2$·2MeCN (794.33): C 36.29, H 5.58, N 10.58; found: C 36.03, H 5.47, N 10.73. Crystals suitable for X-ray analysis were grown from a saturated acetonitrile solution at room temperature.

Preparation of dichloro–manganese and –iron complexes of ligands 10a,b—synthesis of (*S*,*R*,*R*,*S*)-18a(Cl)$_2$: $MnCl_2$ (0.076 g, 0.60 mmol) was added to a solution of (*S*,*R*,*R*,*S*)-**10a** (0.240 g, 0.611 mmol) in MeCN (5 mL). The resulting slightly orange solution was stirred at room temperature overnight. Volatiles were removed in vacuo and THF (5 mL) was added and then evaporated. This procedure was repeated twice to give a colorless solid, which was washed with Et_2O (5 mL) and dried in vacuo; yield: 0.22 g (70%). MS(FAB): *m*/*z* (%): 482 (100) $[M-Cl]^+$; elemental analysis calcd (%) for $C_{22}H_{40}Cl_2MnN_4O_2$ (518.42): C 50.97, H 7.78, N 10.81; found: C 50.73, H 7.91, N 10.42.

Complex (S,R,R,S)-***18b(Cl)$_2$***: $MnCl_2$ (0.1 g, 0.79 mmol), (*S*,*R*,*R*,*S*)-**10b** (0.35 g, 0.83 mmol), MeCN (5 mL), yield: 0.3 g (67%) of colorless solid. MS(FAB): *m*/*z* (%): 510 (100) $[M-Cl]^+$; elemental analysis calcd (%) for $C_{24}H_{44}Cl_2MnN_4O_2$ (546.48): C 52.75, H 8.12, N 10.25; found: C 52.51, H 8.02, N 9.96. Crystals suitable for X-ray analysis were grown in a solution of acetonitrile at room temperature.

Complex (S,R,R,S)-***19a(Cl)$_2$***: $FeCl_2$ (0.046 g, 0.363 mmol), (*S*,*R*,*R*,*S*)-**10a** (0.150 g, 0.382 mmol), MeCN (3 mL), yield: 0.126 g (67%) of a slightly orange solid. MS(FAB): *m*/*z* (%): 483 (100) $[M-Cl]^+$; elemental analysis calcd (%) for $C_{22}H_{40}Cl_2FeN_4O_2$ (519.33): C 50.88, H 7.76, N 10.79; found: C 50.07, H 7.55, N 10.17.

Complex (S,R,R,S)-***19b(Cl)$_2$***: $FeCl_2$ (0.114 g, 0.903 mmol), (*S*,*R*,*R*,*S*)-**10b** (0.4 g, 0.95 mmol), MeCN (4 mL), yield: 0.4 g (81%) of an off-white solid. MS(FAB): *m*/*z* (%): 511 (100) $[M-Cl]^+$; elemental analysis calcd

(%) for $C_{24}H_{44}Cl_2FeN_4O_2$ (547.39): C 52.66, H 8.10, N 10.24; found: C 52.46, H 7.94, N 10.11.

*Complex (*R,R,R,R*)-**21(Cl)$_2$***: $MnCl_2$ (0.081 g, 0.644 mmol), (*R*,*R*,*R*,*R*)-**10a** (0.262 g, 0.667 mmol), MeCN (5 mL), yield: 0.27 g (81%) of a colorless solid. MS(FAB): *m*/*z* (%): 482 (100) $[M-Cl]^+$; elemental analysis calcd (%) for $C_{22}H_{40}Cl_2MnN_4O_2$ (518.42): C 50.97, H 7.78, N 10.81; found: C 51.04, H 7.55, N 10.71.

Preparation of the OTf and SbF_6 salts (*S*,*R*,*R*,*S*)-18a,b, (*S*,*R*,*R*,*S*)-19a,b and (*R*,*R*,*R*,*R*)-21a,b—synthesis of (*S*,*R*,*R*,*S*)-18a(OTf)$_2$: AgOTf (0.104 g, 0.405 mmol) was added to a solution of (*S*,*R*,*R*,*S*)-**18a(Cl)$_2$** (0.11 g, 0.212 mmol) in MeCN (5 mL) at room temperature. The reaction mixture was stirred for 1 d protected from light by aluminum foil. The colorless solid was filtered off and the volatiles removed in vacuo. THF (5 mL) was added and then evaporated. This procedure was repeated twice and the resulting colorless residue was washed with Et_2O; yield: 64 mg (41%). MS(FAB): *m*/*z* (%): 596 (100) $[M-OTf]^+$; elemental analysis calcd (%) for $C_{24}H_{40}F_6MnN_4O_8S_2$·0.5 THF (781.71): C 39.95, H 5.67, N 7.17; found: C 40.06, H 5.63, N 7.52.

*Complex (*S,R,R,S*)-**18a(SbF$_6$)$_2$***: $AgSbF_6$ (0.30 g, 0.873 mmol), (*S*,*R*,*R*,*S*)-**18a(Cl)$_2$** (0.231 g, 0.446 mmol), MeCN (4 mL), yield 270 mg (64%) of a colorless solid. MS(FAB): *m*/*z* (%): 682 (100) $[M-SbF_6]^+$; elemental analysis calcd (%) for $C_{22}H_{40}F_{12}MnN_4O_2Sb_2$·0.5 MeCN·0.5 THF (975.6): C 30.78, H 4.70, N 6.46; found: C 30.85, H 4.87, N 6.12.

*Complex (*S,R,R,S*)-**18b(OTf)$_2$***: AgOTf (0.122 g, 0.476 mmol), (*S*,*R*,*R*,*S*)-**18b(Cl)$_2$** (0.13 g, 0.238 mmol), MeCN (5 mL), yield: 0.1 g (55%) of a colorless solid. MS(FAB): *m*/*z* (%): 624 (100) $[M-OTf]^+$; elemental analysis calcd (%) for $C_{26}H_{44}F_6MnN_4O_8S_2$ (773.72): C 40.36, H 5.73, N 7.24; found: C 40.31, H 5.87, N 7.00.

*Complex (*S,R,R,S*)-**18b(SbF$_6$)$_2$***: $AgSbF_6$ (0.43 g, 1.25 mmol), (*S*,*R*,*R*,*S*)-**18b(Cl)$_2$** (0.35 g, 0.64 mmol), MeCN (7 mL), yield: 0.48 g (75%) of colorless solid. MS(FAB): *m*/*z* (%): 710 (100) $[M-SbF_6]^+$, 494 (86) [(*S*,*R*,*R*,*S*-**10b**)Mn(F)]$^+$; elemental analysis calcd (%) for $C_{24}H_{46}F_{12}MnN_4O_2Sb_2$·2 CH_3CN (1029.2): C 32.68, H 4.90, N 8.17; found: C 32.83, H 4.89, N 8.08.

*Complex (*S,R,R,S*)-**19a(SbF$_6$)$_2$***: $AgSbF_6$ (0.131 g, 0.381 mmol), (*S*,*R*,*R*,*S*)-**19a(Cl)$_2$** (0.1 g, 0.192 mmol), MeCN (5 mL), yield: 0.18 g (95%) of an orange solid. MS(FAB): *m*/*z* (%): 683 (15) $[M-SbF_6]^+$, 467 (17) [(*S*,*R*,*R*,*S*-**10a**)Fe(F)]$^+$; elemental analysis calcd (%) for $C_{22}H_{40}F_{12}FeN_4O_2Sb_2$·$CH_3CN$·0.5 Et_2O (998.04): C 31.29, H 4.85, N 7.02; found: C 31.25, H 4.90, N 7.23.

*Complex (*S,R,R,S*)-**19b(SbF$_6$)$_2$***: $AgSbF_6$ (0.248 g, 0.722 mmol), (*S*,*R*,*R*,*S*)-**19b(Cl)$_2$** (0.2 g, 0.365 mmol), MeCN (4 mL), yield: 270 mg (76%) of a colorless solid. MS(FAB): *m*/*z* (%): 711 (30) $[M-SbF_6]^+$, 495 (100) [(*S*,*R*,*R*,*S*-**10b**)Fe(F)]$^+$; elemental analysis calcd (%) for $C_{24}H_{44}F_{12}FeN_4O_2Sb_2$·$CH_3CN$ (989.03): C 31.57, H 4.79, N 7.08; found: C 31.47, H 4.88, N 7.03.

*Complex (*R,R,R,R*)-**21(OTf)$_2$***: AgOTf (0.114 g, 0.444 mmol), (*R*,*R*,*R*,*R*)-**21(Cl)$_2$** (0.12 g, 0.230 mmol), MeCN (5 mL), yield: 126 mg (76%) of colorless solid. MS(FAB): *m*/*z* (%): 596 (100) $[M-OTf]^+$; elemental analysis calcd (%) for $C_{24}H_{40}F_6MnN_4O_8S_2$ (745.66): C 38.66, H 5.41, N 7.51; found: C 38.90, H 5.46, N 7.38.

Epoxidation procedure: To a solution of alkene (0.2 mmol, 0.2 M) and catalyst (0.01 mmol, 5 mol%, 0.10 mM) in MeCN (1 mL), 1.5 equivalents of 32% peracetic acid (0.3 mmol) were added dropwise over a period of 2 min. After 30 min the mixture was diluted with Et_2O and filtered through a plug of silica gel. Conversion and yields were determined based on internal dodecane as standard by GC analysis (achiral column: Restek Rtx-1701 (0.25 μm, 30 m, 60 kPa He or H_2), chiral columns: β- or γ-CT from Chiraldex). Epoxides were characterized by using NMR spectroscopy and the absolute configurations assigned by comparison with literature data or reference samples.[37,38]

X-ray analyses of 12a, 13a, 16b(PF$_6$)$_2$, 18b, 20, and 21(SbF$_6$)$_2$: The crystals were measured on a Enraf Nonius Kappa CCD diffractometer at 173 K by using graphite-monochromated $Mo_{K\alpha}$-radiation with λ = 0.71073 Å. The COLLECT suite [NoniusCOLLECT][39] has been used for data collection and integration. The structure was solved by direct methods using the program SIR92 [AltamoreSIR92].[40] Least-squares refinement against F was carried out on all non-hydrogen atoms using the program CRYSTALS.[41] Chebychev polynomial weights[42] were used to complete the refinement. CCDC-626347 (**12a**), -626346 (**13a**), -626348 (**16b(PF$_6$)$_2$**), -626349 (**18b**), -626350 (**20**), -626351 (**21(SbF$_6$)$_2$**) contain the supplementary crystallographic data for this paper. These data can be obtained free of charge from the Cambridge Crystallographic Data Center via www.ccdc.cam.ac.uk/data_request/cif.

Acknowledgements

We thank Dr. Axel Franzke and Dr. Clément Mazet for 500 MHz NMR spectra. Financial support by the Swiss National Science Foundation is gratefully acknowledged.

[1] *Biomimetic Oxidations Catalyzed by Transition Metal Complexes* (Ed.: B. Meunier), Imperial College Press, London (UK), **2000**.

[2] a) *Cytochrome P450: Structure, Mechanism, and Biochemistry*, 2nd ed. (Ed.: P. R. Ortiz de Montellano), Plenum Press, New York, **1995**; b) B. Meunier, S. P. de Vissier, S. Shaik, *Chem. Rev.* **2004**, *104*, 3947–3980.

[3] a) J. T. Groves, T. E. Nemo, R. S. Myers, *J. Am. Chem. Soc.* **1979**, *101*, 1032–1033; b) I. Tabushi, N. Koga, *J. Am. Chem. Soc.* **1979**, *101*, 6456–6458; c) E. Guilmet, B. Meunier, *Tetrahedron Lett.* **1980**, *21*, 4449–4450.

[4] a) S. I. Murahashi, T. Naota in *Comprehensive Organometallic Chemistry II: A Review of the Literature 1982–1994, Vol. 12* (Eds.: E. W. Abel, F. G. A. Stone, G. Wilkinson), Pergamon, Oxford (UK), **1995**, Chapter 11.3; b) *The Porphyrin Handbook* (Eds.: K. M. Kadish, K. M. Smith, R. Guilard), Academic, New York, **2000**.

[5] E. N. Jacobsen in *Comprehensive Organometallic Chemistry II: A Review of the Literature 1982–1994, Vol. 12* (Eds.: E. W. Abel, F. G. A. Stone, G. Wilkinson), Pergamon, Oxford (UK), **1995**, Chapter 11.1, pp. 1097–1135.

[6] a) W. Zhang, J. L. Loebach, S. R. Wilson, E. N. Jacobsen, *J. Am. Chem. Soc.* **1990**, *112*, 2801–2803; b) R. Irie, K. Noda, Y. Ito, N. Matsumoto, T. Katsuki, *Tetrahedron Lett.* **1990**, *31*, 7345–7348; c) E. M. McGarrigle, D. G. Gilheany, *Chem. Rev.* **2005**, *105*, 1563–1602.

[7] a) B. J. Wallar, J. D. Lipscomb, *Chem. Rev.* **1996**, *96*, 2625–2658; b) E. Y. Tshuva, S. J. Lippard, *Chem. Rev.* **2004**, *104*, 987–1012.

[8] a) E. Carredano, A. Karlsson, B. Kauppi, D. Choudhury, R. E. Parales, J. V. Parales, K. Lee, D. T. Gibson, H. Eklund, S. Ramaswamy, *J. Mol. Biol.* **2000**, *296*, 701–712; b) A. Karlsson, J. V. Parales, R. E. Parales, D. T. Gibson, H. Eklund, S. Ramaswamy, *Science* **2003**, *299*, 1039; c) M. Costas, M. P. Mehn, M. P. Jensen, L. Que, Jr., *Chem. Rev.* **2004**, *104*, 939–986.

[9] a) A. Murphy, G. Dubois, T. D. P. Stack, *J. Am. Chem. Soc.* **2003**, *125*, 5250–5251; b) A. Murphy, A. Pace, T. D. P. Stack, *Org. Lett.* **2004**, *6*, 3119–3122; c) A. Murphy, T. D. P. Stack, *J. Mol. Catal. A* **2006**, *251*, 78–88.

[10] a) M. C. White, A. G. Doyle, E. N. Jacobsen, *J. Am. Chem. Soc.* **2001**, *123*, 7194–7195; b) C. Copéret, H. Adolfsson, K. B. Sharpless, *Chem. Commun.* **1997**, 1565–1566; c) K. Sato, M. Aoki, M. Ogawa, T. Hashimoto, R. Noyori, *J. Org. Chem.* **1996**, *61*, 8310–8311; d) B. S. Lane, K. Burgess, *Chem. Rev.* **2003**, *103*, 2457–2473.

[11] For chiral Ru catalysts with other types of pyridine-based ligands, see: M. K. Tse, S. Bhor, M. Klawonn, G. Anilkumar, H. Jiao, A. Spannenberg, C. Döbler, W. Mägerlein, H. Hugl, M. Beller, *Chem. Eur. J.* **2006**, *12*, 1875–1888; for Mn catalysts derived from chiral 1,4,7-triazacyclononane, see: K. F. Sibbons, K. Shastri, M. Watkinson, *Dalton Trans.* **2006**, 645–661.

[12] a) A. Pfaltz, *Synlett* **1999**, 835–842; b) G. Helmchen, A. Pfaltz, *Acc. Chem. Res.* **2000**, *33*, 336–345; c) A. Pfaltz, W. J. Drury III, *Proc. Natl. Acad. Sci. USA* **2004**, *101*, 5723–5726; d) N. End, L. Macko, M. Zehnder, A. Pfaltz, *Chem. Eur. J.* **1998**, *4*, 818–824; N. End, A. Pfaltz, *Chem. Commun.* **1998**, 589–590.

[13] For a review on chiral oxazoline ligands, see: H. A. McManus, P. J. Guiry, *Chem. Rev.* **2004**, *104*, 4151–4202.
[14] a) M. D. Wittman, J. Kallmerten, *J. Org. Chem.* **1988**, *53*, 4631–4633; b) K. Kamata, H. Sato, E. Takagi, I. Agata, A. I. Meyers, *Heterocycles* **1999**, *51*, 373–378.
[15] a) A. I. Meyers, G. Knaus, P. M. Kendall, *Tetrahedron Lett.* **1974**, *15*, 3495–3498; b) P. Breton, C. Andre-Barres, Y. Langlois, *Synth. Commun.* **1992**, *22*, 2543.
[16] T. A. Chamberlin, US-A 3962235, **1996** [*Chem. Abstr.* **1976**, *85*, 160113x].
[17] K. Kamata, I. Agata, A. I. Meyers, *J. Org. Chem.* **1998**, *63*, 3113–3116.
[18] S. Nanchen, A. Pfaltz, *Chem. Eur. J.* **2006**, *12*, 4550–4558.
[19] Similar conditions have been used for the preparation of related bisoxazoline ligands derived from 1,5-diazacyclooctane: Z.-L. Shang, Z.-C. Shang, Q.-S. Yu, *Synth. Commun.* **2002**, *32*, 3461–3464.
[20] For fluorine transfer reactions of this type, see: a) R. F. Jordan, W. E. Dasher, S. F. Echols, *J. Am. Chem. Soc.* **1986**, *108*, 1718–1719; b) J. Reedijk, *Comments Inorg. Chem.* **1982**, *1*, 379–389.
[21] For related neutral N_2Py_2 ligands, see: P. A. Goodson, J. Glerup, D. J. Hodgson, K. Michelsen, H. Weihe, *Inorg. Chem.* **1991**, *30*, 4909–4914.
[22] N. Arulsamy, D. J. Hodgson, J. Glerup, *Inorg. Chim. Acta* **1993**, *209*, 61–69.
[23] P. A. Goodson, J. Glerup, D. J. Hodgson, K. Michelsen, U. Rychlewska, *Inorg. Chem.* **1994**, *33*, 359–366.
[24] J. Glerup, P. A. Goodson, A. Hazell, R. Hazell, D. J. Hodgson, C. J. McKenzie, K. Michelsen, U. Rychlewska, H. Toftlund, *Inorg. Chem.* **1994**, *33*, 4105–4111.
[25] K. Chen, L. Que, Jr., *Chem. Commun.* **1999**, *15*, 1375–1376.
[26] J. Simaan, S. Poussereau, G. Blondin, J.-J. Girerd, D. Defaye, C. Philouze, J. Guilhem, L. Tchertanov, *Inorg. Chim. Acta* **2000**, *299*, 221–230, and references therein.
[27] Y. Mekmouche, S. Ménage, C. Toia-Duboc, M. Fontecave, J.-B. Galey, C. Lebrun, J. Pécaut, *Angew. Chem.* **2001**, *113*, 975–978; *Angew. Chem. Int. Ed.* **2001**, *40*, 949–952.
[28] K. Chen, M. Costas, J. Kim, A. K. Tipton, L. Que, Jr., *J. Am. Chem. Soc.* **2002**, *124*, 3026–3035.
[29] V. Balland, F. Banse, E. Anxolabéhère-Mallart, M. Nierlich, J.-J. Girerd, *Eur. J. Inorg. Chem.* **2003**, 2529–2535.
[30] R. Mas-Ballesté, M. Costas, T. van den Berg, L. Que, Jr., *Chem. Eur. J.* **2006**, *12*, 7489–7500, and references therein.
[31] For diamine-diimidazole ligands, see: S. Poussereau, G. Blondin, G. Chottard, J. Guilhem, L. Tchertanov, E. Rivière, J.-J. Girerd, *Eur. J. Inorg. Chem.* **2001**, 1057–1062.
[32] For related diamine-diamide ligands, see: J.-F. Carpentier, A. Martin, D. C. Swenson, R. F. Jordan, *Organometallics* **2003**, *22*, 4999–5010.
[33] M. Costas, A. K. Tipton, K. Chen, D.-H. Jo, L. Que, Jr., *J. Am. Chem. Soc.* **2001**, *123*, 6722–6723.
[34] A. W. Addison, T. N. Rao, J. Reedijk, J. van Rijn, G. C. Verschoor *J. Chem. Soc., Dalton Trans.* **1984**, 1349.
[35] W. L. F. Armarego, D. D. Perrin, *Purification of Laboratory Chemicals*, 4th ed., Butterworth-Heinmann, Oxford, **1996**.
[36] P. Kapron, G. Lhommet, P. Maitte, *Tetrahedron Lett.* **1981**, *22*, 2255–2258.
[37] N. End, PhD Thesis, University of Basel (Switzerland), **1997** and ref. [12c].
[38] Z. Wang, L. Shu, M. Frohn, Y. Tu, Y. Shi, *Org. Synth.* **2003**, *80*, 9–17.
[39] B. V. Nonius, COLLECT Software, 1997–2001.
[40] A. Altomare, G. Cascarano, G. Giacovazzo, A. Guagliardi, M. C. Burla, G. Polidori, M. Camalli: SIR92 - A Program for Automatic Solution of Crystal Structures by Direct Methods, *J. Appl. Crystallogr.* **1994**, *27*, 435.
[41] P. W. Betteridge, J. R. Carruthers, R. I. Cooper, K. Prout, D. J. Watkin, *J. Appl. Cryst.* **2003**, *36*, 1487.
[42] a) E. Prince in *Mathematical Techniques in Crystallography and Materials Science*, Springer, New York, **1982**; b) D. J. Watkin, *Acta Crystallogr. Sect. A* **1994**, *50*, 411–437.

Received: May 31, 2007
Published online: August 23, 2007

